Dynamic Response Measurements and Identification Analysis of a Pavement During Falling-Weight Deflectometer Experiments

STEPHEN A. KETCHAM

Falling-weight deflectometer (FWD) experiments were conducted on an airport taxiway pavement using techniques of experimental dynamics to obtain compliance frequency response functions of the pavement, which are functions in the frequency domain that represent the pavement displacement response at a given location to the FWD load. The compliance functions reveal that at certain locations the pavement responded to the FWD load with a significant resonant amplification at approximately 30 Hz. To understand this response and to develop appropriate techniques for backcalculation when dynamic behavior should not be ignored, the compliance data were used to backcalculate selected pavement properties using a minimization algorithm and a wave propagation model applicable to pavement systems. The backcalculations provide a credible explanation of the observed pavement behavior. They also demonstrate the utility of the minimization algorithm and wave propagation model to estimate pavement system properties using dynamic response data from FWD tests.

A falling-weight deflectometer (FWD) is an apparatus for testing pavements. FWD experiments are performed by dropping a mass onto a circular pad, measuring the force history of the drop, and measuring the vertical velocity response of the pavement surface at several distances from the load center. Peak-load and peak-displacement values are calculated from the measured transient load and velocity histories of an experiment. These values are often used by pavement engineers as quasi-static response data to match in elastic modulus identification calculations using a static model of the pavement system. This process is generally referred to as "backcalculation."

Several investigators have suggested that the inertial and dissipative responses can contribute significantly to the load and velocity responses measured during FWD experiments; that is, the dynamics of an FWD test can be important. Roesset and Shao (*1*), Sebaaly et al. (*2*), Anderson (*3*), Magnuson et al. (*4*), and Chang et al. (*5*) have conducted studies of the dynamic response of pavements to understand the implications of the static assumption on backcalculation results. Roesset and Shao (*1*) and Chang et al. (*5*) have shown that a pavement system with a bedrock or other relatively hard layer at shallow depth can have resonant vibration modes that may be excited during FWD experiments. They have suggested that the use of static backcalculation techniques can lead to erroneous results because of their inability to account for an amplified, dynamic response. Their studies indicate that the quasi-static assumption inherent in conventional FWD backcalculation practice should be further evaluated.

This paper presents results from FWD experiments of a pavement that responded at a number of locations with a significant resonant vibration at approximately 30 Hz, and at other locations without this distinct resonance. To quantify the dynamic response, the experiments were conducted with supplemental instrumentation and the data were analyzed using conventional signal processing techniques of experimental dynamics. A minimization algorithm (*6*) together with a wave propagation model applicable to pavements (*7,8*) were used to backcalculate selected pavement layer properties from the experimental data sets. The identified models provide a credible explanation of the resonant response behavior of the pavement, and the analysis demonstrates that the method is appropriate for backcalculation when rigid or relatively hard layers underlie the pavement structure.

EXPERIMENTAL TECHNIQUE AND RESULTS

The tests reported here were conducted April 11, 1991, at the Lebanon, New Hampshire, Airport at three locations on taxiway B. A Dynatest 8000 FWD with a 30-cm-diameter load plate was used as the loading system together with an array of accelerometers and a dynamic data acquisition system as the response measurement system. Experiments were conducted by recording the load cell and displacement histories provided by the FWD system and the response histories of the accelerometers.

Pavement System and Experimental Configuration

The taxiway pavement was 15.2 m wide and consisted of 12.7 cm of asphalt concrete surface course over 15.2 cm of crushed aggregate base course, approximately 1 m of subbase course, and subgrade. Instrumentation at the site indicated that the pavement soil was unfrozen and had thawed completely several weeks prior to the test date. The design thickness of the subbase course was 94 cm, but the constructed thickness was

U.S. Army Engineer Cold Regions Research and Engineering Laboratory, 72 Lyme Road, Hanover, N.H. 03755-1290.

slightly greater at some locations according to construction documents. The additional depth was unknown at the test locations.

The tests were conducted along the center line of the taxiway at locations 60 m apart. The taxiway runs approximately southwest to northeast. The test location furthest to the southwest was designated station 18-00 on the taxiway construction drawings; the middle location was designated 20-00; and the location furthest to the northeast was designated 22-00. (These designations were based on the distance in feet from the beginning of the taxiway.) Information from a site investigation pit close to the 20-00 location that was excavated prior to construction indicated that the subgrade was a "very dense gravelly silty sand." The depth of the pit was 3.6 m. Information from borings much further from the test locations indicated that the depth to bedrock was likely to be greater than 10 m at the sites.

The accelerometers were attached to the pavement surface at the radial distances 0.30, 0.45, 0.75, 1.05, and 2.25 m from the load pad center, and the geophones of the FWD system were located at distances of 0, 0.305, 0.61, 0.91, 1.22, 1.52, and 1.83 m. All were oriented to measure vertical responses.

Data Analysis

A set of specifications for a digitally sampled signal is the sampling interval Δt, which is the time domain resolution, and the duration of sampling T. The number of samples (N) is

$$N = \frac{T}{\Delta t} \tag{1}$$

The highest frequency that will appear in the sampled data (f_c) is called the Nyquist frequency. The Nyquist frequency is

$$f_c = \frac{1}{2\Delta t} \tag{2}$$

The frequency domain resolution is the bandwidth Δf, that is,

$$\Delta f = \frac{1}{T} = \frac{1}{N\Delta t} \tag{3}$$

The sampling rate is the frequency $1/\Delta t$, which is twice the Nyquist frequency. The sampling rate used for this study (5,000 Hz) was dictated by the sampling rate of the FWD load cell output, which was not adjustable. The Nyquist frequency corresponding to this sampling rate is 2,500 Hz. The number of values of the accelerometer data sequences is 2,048, which corresponds to a sample duration of approximately 0.41 sec and a frequency resolution of approximately 2.44 Hz. The number of values and the sample duration of the FWD data acquisition system were 300 and 0.06 sec, respectively, and these were not adjustable. The accelerometers and the dynamic data acquisition system were used as an alternative to the FWD geophones and measurement system specifically because the 0.06 sec sample duration of the FWD system was not long enough to capture the complete response of the pavement and would have been unnecessary if the FWD sample duration could have been set to a sufficient duration.

The load and acceleration histories of the repetitions were used to calculate frequency response and impulse response functions between the load and response, according to conventional linear systems-based analysis techniques for dynamic testing of structures (*9,10*). An impulse response function $h(t)$ of a structure relates a structural response $y(t)$ to a loading history $x(t)$ by the convolution integral

$$y(t) = \int_{-\infty}^{\infty} h(\tau)x(t - \tau)d\tau \tag{4}$$

and a frequency response function $H(f)$ relates the Fourier transform of the structural response $Y(f)$ to the Fourier transform of the loading history $X(f)$ by the multiplication

$$Y(f) = H(f)X(f) \tag{5}$$

where t and f denote the time and frequency domains, respectively. Frequency response and impulse response functions make up a Fourier transform pair. For digital signals, discrete versions of Equations 4 and 5 apply.

A frequency response function is complex valued. It can be illustrated by plotting the real and imaginary components of the function versus frequency as well as by plotting the amplitude (termed gain) and phase angle versus frequency. The physical significance of a frequency response function can be thought of as follows: If a linear system were excited with a sinusoidal input of unit amplitude, the response would be sinusoidal with the same frequency as the input, and it would have an amplitude that is given by the gain value and a phase lag that is given by the phase angle. The static response of the system would be given by the 0-Hz value of the amplitude or the real component.

For a pavement system excited with an FWD load, a frequency response function for a given measurement location can be calculated simply as the Fourier transform of the response signal divided by the Fourier transform of the load signal, as suggested by Equation 5. However, considering the influence of measurement noise and the random error that is inherent in frequency response estimates, an equation for an optimal calculation of a frequency response function for the pavement system, using averaged results from a number of FWD experiments, is (*9*)

$$H(f) = \frac{\bar{S}_{xy}(f)}{\bar{S}_{xx}(f)} \tag{6}$$

where

$\bar{S}_{xy}(f)$ = averaged energy cross-spectral density function between load input signals (subscript x) and motion output signals (subscript y),
$\bar{S}_{xx}(f)$ = averaged energy autospectral density function of the load input signals, and
f = discrete frequency sequence.

For a single test record, these functions are related to the Fourier transforms of the load input and motion output sig-

nals, $X(f)$ and $Y(f)$, respectively, by

$$S_{xy}(f) = X^*(f)Y(f) \tag{7}$$

and

$$S_{xx}(f) = X^*(f)X(f) \tag{8}$$

where the asterisk indicates the complex conjugate. For n FWD test repetitions, the averaged functions are calculated by

$$\bar{S}_{xy}(f) = \frac{1}{n}\sum_{i=1}^{n} S_{xy_i}(f) \tag{9}$$

and

$$\bar{S}_{xx}(f) = \frac{1}{n}\sum_{i=1}^{n} S_{xx_i}(f) \tag{10}$$

Eight FWD test repetitions were conducted for the experiments reported here so that the averaging technique of these equations could be followed.

Because the measured signals in this study were force and acceleration histories, "accelerance" frequency-response functions, that is, frequency-response functions relating force inputs and acceleration outputs, were calculated directly from the experimental results. However, of greater interest for the pavement response interpretations in this study were "compliance" functions, or frequency-response functions relating force inputs and displacement response outputs. Compliance functions are inverses of "dynamic stiffness," and reflect the mass, damping, and stiffness response characteristics of a structure. These functions were calculated from the accelerance functions by frequency domain integration. Although the frequency response function calculations are based on linear systems theory, the material responses of pavement systems are inherently nonlinear. For transient excitations such as FWD loads, using Equation 6 results in an equivalent linear estimate of the accelerance or compliance function at a given load level (*11*).

Measurements and Pavement Response Functions

Measurements and data analysis results from the tests at station 20–00 are presented in Figures 1, 2, and 3. The measurements are from the first repetition of the tests. Force and displacement histories from the FWD data acquisition system are presented in Figure 1, and acceleration histories are presented in Figure 2. Although the acceleration signals are shown only to 0.1 sec, the 0.41-sec sample duration allowed the full response transient of the initial FWD load "bounce" to be captured. Of particular interest in this study are the damped oscillations of the displacement and acceleration signals after the load is completely removed. These oscillations indicate that the dynamic response of the pavement is significant.

Compliance functions that were calculated from the load and acceleration measurements are depicted in Figure 3 over the 7- to 200-Hz bandwidth. The functions are presented in a gain and phase format. Data below 7 Hz were unavailable because the test was a dynamic loading test such that the low frequency loading and response of the pavement system was small. The experimental consequence was a low signal-to-

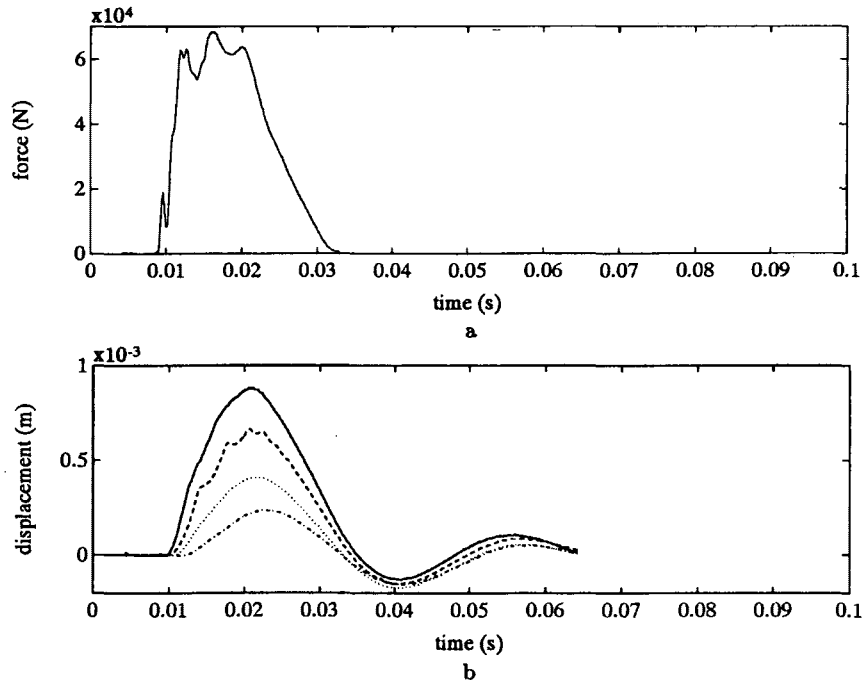

FIGURE 1 Data of first test at location 20-00: (*a*) FWD force history; (*b*) FWD displacement histories from geophones located at 0 m (*solid line*), 0.305 m (*dashed line*), 0.61 m (*dotted line*), and 0.91 m (*dash-dot line*) from load center.

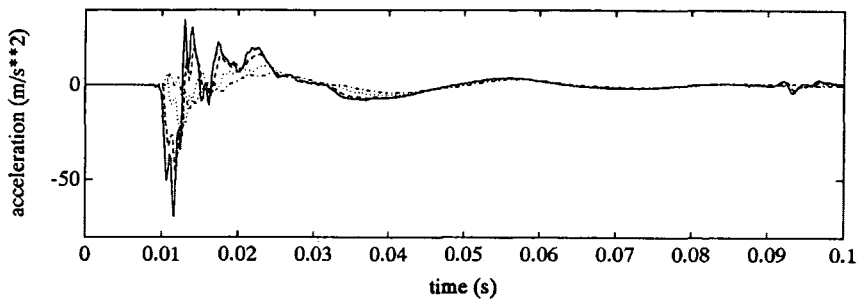

FIGURE 2 Data of first test at location 20-00, acceleration histories from accelerometers located at 0.30 m (*solid line*), 0.45 m (*dashed line*), 0.75 m (*dotted line*), and 1.05 m (*dash-dot line*) from FWD load center.

noise ratio below 7 Hz, which produced errors in the calculated spectral quantities in this bandwidth. The gain spectra contained appreciable peaks around 30 Hz, which indicated that the FWD load excited a resonance of the pavement system. The dominance of the resonance, together with the damped oscillations of the displacement and acceleration histories after the load is zero, provided an experimental indication that the dynamic response of this pavement system should not be ignored for backcalculation of properties.

Bias errors were present in the compliance function estimates as a result of the experimental technique. In particular, the load and accelerometer signals were not synchronous because they were measured using different data acquisition systems, and this introduces an unknown error into the compliance function estimates. An improved measurement system would allow synchronous measurements while providing complete motion responses. In addition, because the tires of the FWD trailer are unloaded when the weight is dropped, the measured load is not the entire disturbance of the pavement.

Compliance functions calculated from measurements of the tests at locations 18-00 and 22-00 are shown in Figure 4 together with a compliance function from location 20-00. These functions reveal a pavement response behavior that is similar to the behavior at station 20-00. The nature of this behavior is examined in the following section.

SYSTEM IDENTIFICATION TECHNIQUE AND RESULTS

A system identification technique based partly on the method presented by Luco and Wong (*12*) for estimating soil properties from dynamic responses of foundations was used for this study. With this technique, pavement system properties were

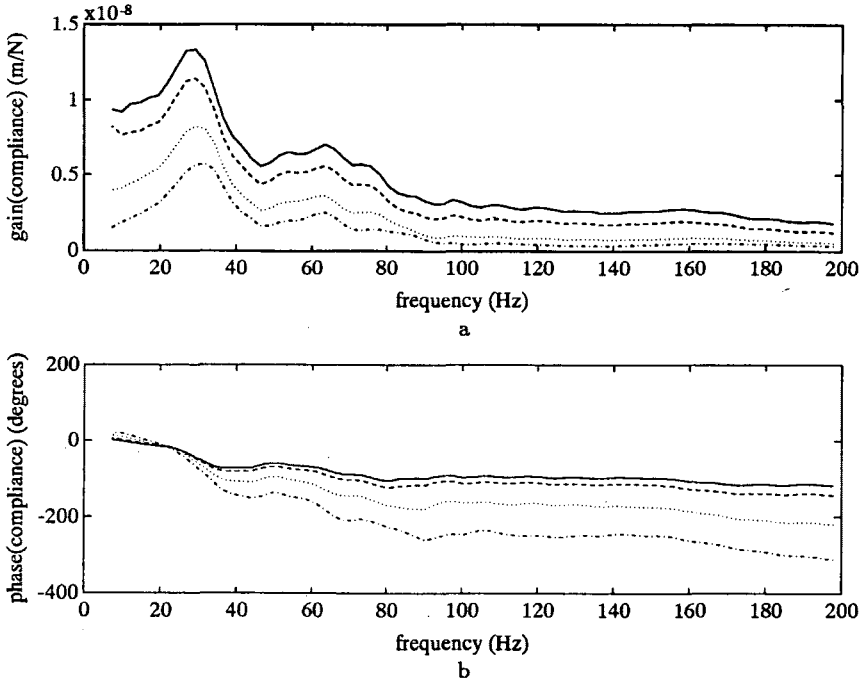

FIGURE 3 Compliance functions for location 20-00 corresponding to locations at 0.30 m (*solid line*), 0.45 m (*dashed line*), 0.75 m (*dotted line*), and 1.05 m (*dash-dot line*) from FWD load center: (*a*) gain spectra; (*b*) phase spectra.

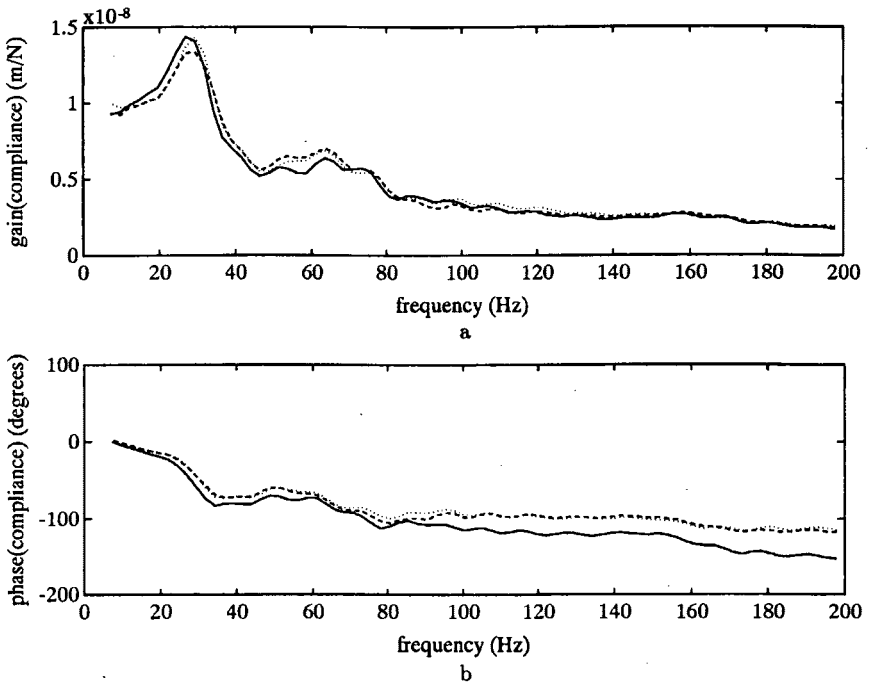

FIGURE 4 Compliance functions for stations 18-00 (*solid line*) and 22-00 (*dotted line*) together with a compliance function from station 20-00 (*dashed line*) for a location 30 cm from FWD load center: (*a*) gain spectra; (*b*) phase spectra.

estimated by minimizing a relative error function that quantifies the difference between compliance function data predicted by a wave propagation model for an FWD test and the experimentally derived compliance functions presented above. The minimization was performed using a "quasi-Newton" algorithm (*6,13*) to vary selected input properties of the model. Real and imaginary data components of the experimental and model compliance functions at selected frequencies were used to calculate the error measure. The wave propagation model is the "thin layer method" described by Kausel and Peek (*7*) and Seale and Kausel (*8*).

The thin layer method is an algorithm for modeling the response of a layered elastic system with hysteretic damping to a dynamic load. It assumes layering of infinite horizontal extent. It has been used by several investigators (*1–3,5*) for FWD pavement response predictions. The thin layer method is a state-of-the-art technique for modeling dynamic pavement response.

Software implementation of the thin layer algorithm (*14*) includes coding of (*a*) the input of elastic constants, mass density, hysteretic damping ratio, thickness for each layer, and the harmonic loading frequency; (*b*) the formation of a wavenumber domain stiffness matrix for the system; (*c*) the solution of the eigenproblem, which provides modes of wave propagation in the form of eigenvalues and eigenvectors; and (*d*) the superposition of the modal solutions for a given load configuration (*7*) for each output location, which may be at any specific radius and layer interface combination. Step d provides the compliance values at the input frequency, and steps b, c, and d are repeated for each harmonic of interest to obtain compliance spectra. The software implementation used for this study is the program PUNCH written by Kausel (*15*). This program can be used to model a vertical, circular, and uniform load in an axisymmetric context, which is applicable to the loading and displacement response of an FWD experiment. The halfspace approximation of Seale and Kausel (*8*) is incorporated so that models of a pavement system over a halfspace can be analyzed.

Analysis and Results

Using the compliance data from location 20-00, an identification analysis was conducted by assuming that an idealized thin layer model of the loading and pavement system could capture predominant features of the experimental compliance functions. In particular, it was assumed that the FWD load was uniform over the area of the loading pad, that the pavement surface course, base course, subbase course, and subgrade are each homogeneous in material properties, and that the material properties do not change significantly across the dominant frequency bandwidth of the FWD load. It was also assumed that the subgrade could be represented by a halfspace. Results from a single analysis are presented here. In the analysis, 13 pavement system properties were selected for identification: the shear moduli, hysteretic damping ratios and Poisson's ratios of the four pavement layers, and the thickness of the subbase course. The subbase thickness was allowed to vary because, as mentioned, the actual constructed thickness is unknown and because the thickness as well as the shear modulus of the subbase course was expected to have predominantly influenced the observed resonant behavior. Maximum and minimum constraints were imposed on the varying properties. Other system properties were held constant throughout the identification iterations.

Compliance function data from the five accelerometer locations and at eleven frequencies were used for the identification analyses. The frequencies that were selected are 9.8, 12.2, 14.6, 17.1, 22.0, 26.8, 31.7, 41.5, 56.1, 75.7, and 100.1 Hz, which are concentrated primarily at the lower frequency end of the spectra and around the resonant feature. The initial property guesses and assumed system constants for the analysis are presented in Table 1. Identification results are presented in Table 2 and in Figures 5, 6, 7, and 8. In Figure 5, compliance values of the model that were based on the initial guesses and assumed constants of Table 1 are shown relative to the experimental functions. The bandwidth of the spectra in this figure is 7 to 117 Hz. It is clear from Figure 5 that the initial guesses are not a good set of properties for this pavement.

In Figure 6 the variations of layer shear moduli, hysteretic damping ratios, Poisson's ratios, and subbase thickness with iteration number are shown. The maximum and minimum constraints were reached only in the variation of the subbase thickness, and these were 1.17 m and 0.94 m, respectively. As indicated in Figure 6, the Poisson's ratios were held constant until Iteration 24.

In Figure 7 the variation of the relative error measure is shown. The relative error was calculated at the sum of the squares of the differences between the model and experimental compliance values, divided by the sum of the squares of the model values. The relative error reached a minimum at Iteration 23 with the Poisson's ratios held constant, and at Iteration 47 with all properties varying.

Figure 8 illustrates the final compliance values of the model relative to the experimental functions. It can be observed that the dominant resonant feature of the compliance functions is captured by the identified model, even though a simple layered system underlain by a halfspace was used to represent the pavement. The estimated values for the varied properties are given in Table 2. Of particular interest for understanding the resonant response are the shear moduli and the subbase thickness. The subbase thickness is a reasonable value close to the design thickness and the shear moduli appear to be reasonable values as well. The latter values quantify the modulus of the "very dense, gravelly silty sand" subgrade, relative to the base and subbase moduli, that is required to cause the resonance.

The compliance spectra of the identified model are shown together with the experimental compliance spectra in Figure 9. The model spectra were calculated using the thin layer method and the identified pavement system properties. The comparison reveals that, as should be expected, the identified model does not capture all features of the experimental compliance spectra. To illustrate the significance of the difference, the identified model was used to predict the pavement displacement response to the FWD load history shown in Figure 1. A comparison of the predicted displacement history for the

TABLE 1 Initial Guesses and Assumed Constants for Identification Analysis, Pavement Location 20-00

layer	h (m)	ρ (kg/m^3)	G (GPa)	ν	D
surface	0.127	2300	(1)	(0.3)	(0.02)
base	0.152	2200	(0.01)	(0.3)	(0.02)
subbase	(1)	1900	(0.01)	(0.3)	(0.02)
subgrade	∞	2100	(0.1)	(0.3)	(0.02)

Symbols: h = layer thickness; ρ = mass density; G = shear modulus; ν = Poisson's ratio; D = hysteretic damping ratio.

Notes: Initial guesses of varying properties are shown in parentheses; Poisson's ratio was not allowed to vary until iteration 24; one discrete layer each was used to model the surface course and the base course; four discrete layers were used to model the subbase course; the subgrade was modeled as four discrete layers in the upper 2 m over a halfspace approximation.

TABLE 2 Backcalculated Values of Pavement System Properties, Pavement Location 20-00

layer	h (m)	G (GPa)	ν	D
surface		3.2	0.30	0.024
base		0.039	0.31	0.021
subbase	0.96	0.018	0.37	0.036
subgrade		0.085	0.43	0.018

Symbols: h = layer thickness; G = shear modulus; ν = Poisson's ratio; D = hysteretic damping ratio.

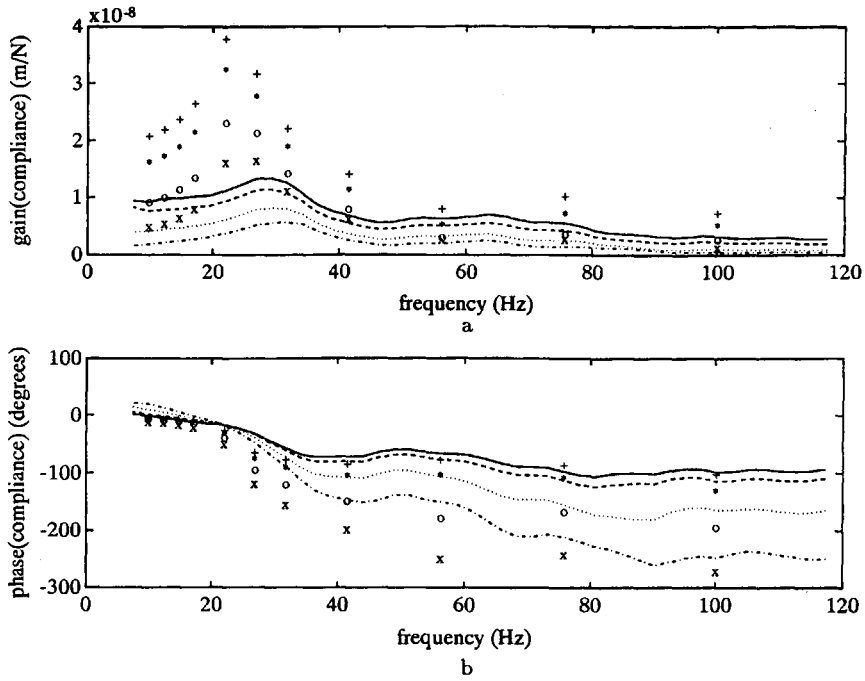

FIGURE 5 Initial compliance values of model relative to experimental compliance spectra for locations at 0.30 m (+, model; *solid line*, experimental), 0.45 m (*, model; *dashed line*, experimental), 0.75 m (○, model; *dotted line*, experimental), and 1.05 m (×, model; *dash-dot line*, experimental) from FWD load center: (*a*) gain spectra; (*b*) phase spectra.

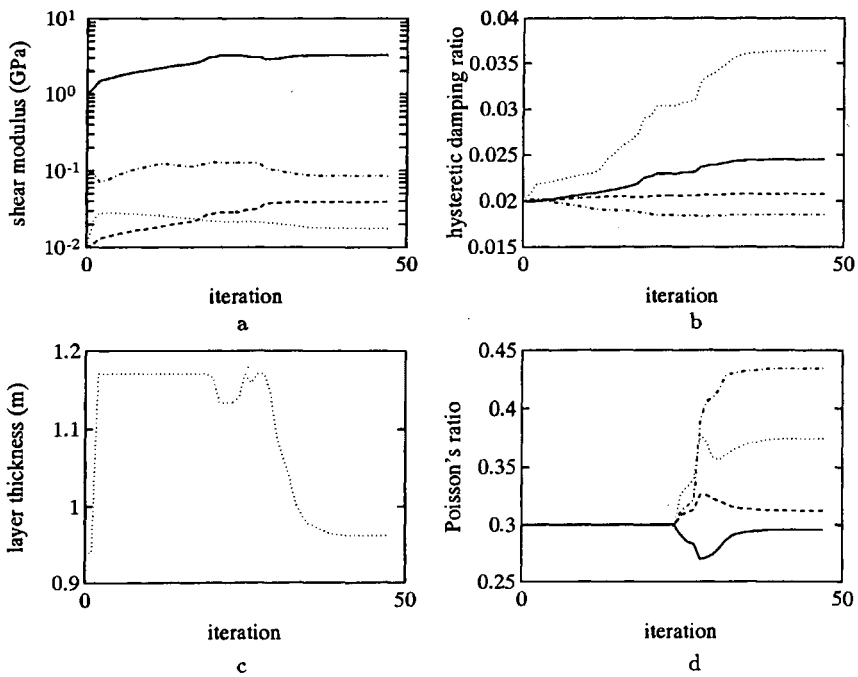

FIGURE 6 Variation of (*a*) shear moduli, (*b*) hysteretic damping ratios, (*c*) layer thickness, and (*d*) Poisson's ratios with iteration number during identification analysis. *Solid line*, surface course; *dashed line*, base course; *dotted line*, subbase course; *dash-dot line*, subgrade.

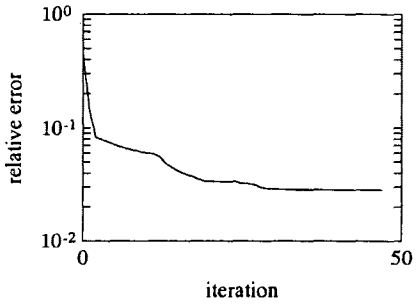

FIGURE 7 Variation of relative error with iteration number.

radial distance 30 cm from the load center with the measured history from the FWD geophone at 30.5 cm is shown in Figure 10. Also shown in this figure are the predicted and measured load versus displacement responses. The comparisons are very favorable and show that the identified model can capture the pavement displacement response to an FWD load, including the damped oscillations after the load is removed, and do so over the complete duration of the transient response. The accuracy of the predictions demonstrates that the identified model is indeed a credible model of the pavement system.

The identified model was further used to predict the static compliance of the pavement as a function of the radial distance from the load center; i.e., the static "deflection basin." This prediction is shown in Figure 11 together with the deflection basin values calculated from the peak load and displacement values from the load cell and geophone data of an FWD test. The figure shows that the deflection basin calculated from the FWD test data is significantly and consistently greater than the static deflection basin calculated from the identified model of the pavement. The comparison suggests that, for this pavement system, the FWD deflection basin should not be used to backcalculate properties using a static pavement system model.

CONCLUSION

The experiments and identification analysis described here comprise the steps of a backcalculation technique that incorporates the dynamic response of the pavement to the FWD load. In practice, this or a similar technique would be a valid backcalculation technique when the peak dynamic displacement during an FWD test is not a good estimate of the static pavement response, that is, when the quasi-static assumption inherent in conventional backcalculation practice is not correct. As several investigators have reported, this can be the case when a pavement is underlain by a rigid or relatively hard layer. This can also be true for cold climate pavements during spring thaw, when a soft thawing soil layer can exist above a hard frozen layer. It is this condition and the need for backcalculation techniques that can be applied to results of FWD tests during spring thaw that have motivated this work. Further developments of FWD backcalculation techniques for cold climate pavements should consider dynamic pavement response and its seasonal variation.

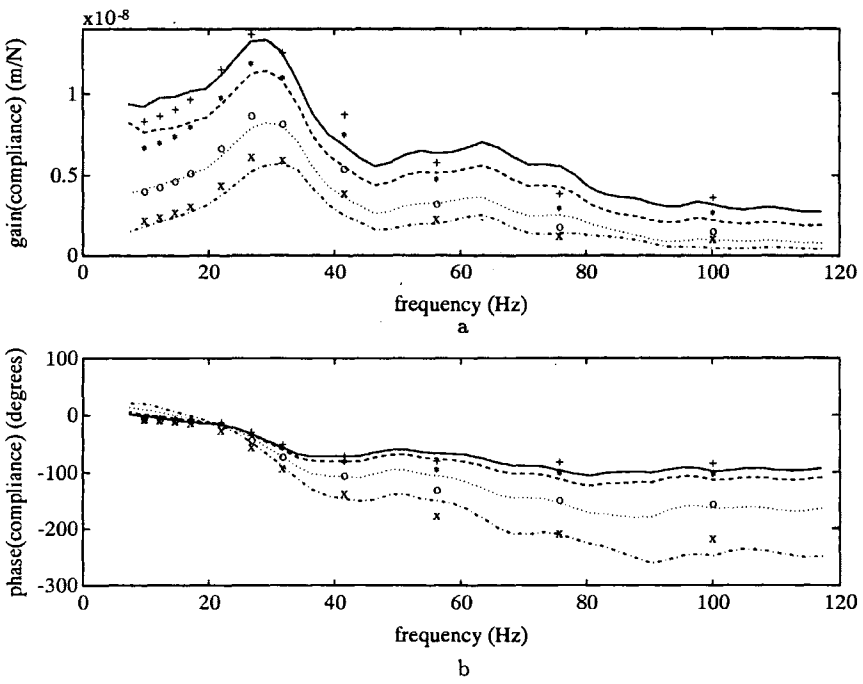

FIGURE 8 Final compliance values of model relative to experimental compliance spectra for locations at 0.30 m (+, model; *solid line*, experimental), 0.45 m (*, model; *dashed line*, experimental), 0.75 m (○, model; *dotted line*, experimental), and 1.05 m (×, model; *dash-dot line*, experimental) from FWD load center: (*a*) gain spectra; (*b*) phase spectra.

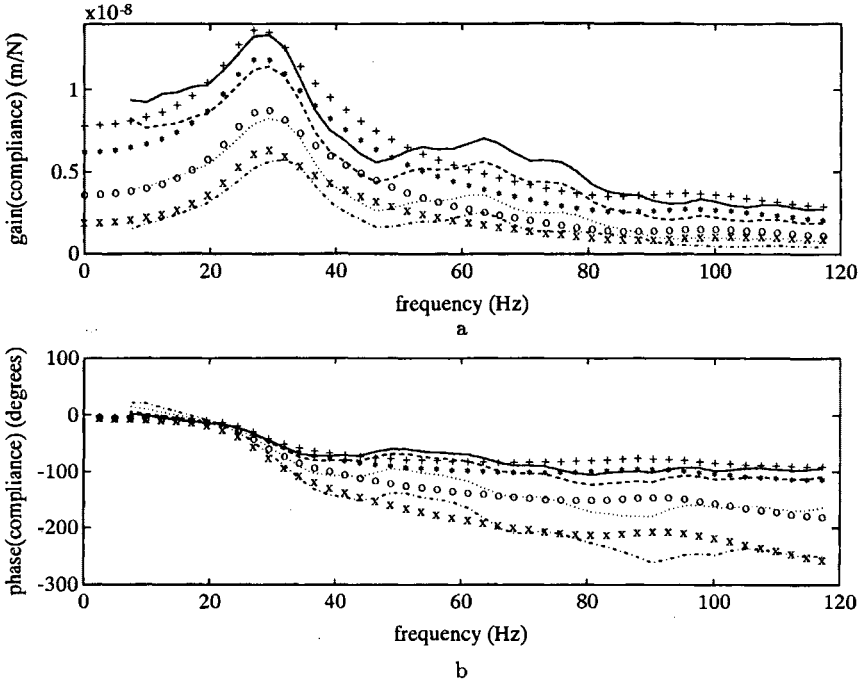

FIGURE 9 Compliance spectra identified model relative to the experimental spectra for locations at 0.30 m (+, model; *solid line*, experimental), 0.45 m (*, model; *dashed line*, experimental), 0.75 m (○, model; *dotted line*, experimental), and 1.05 m (×, model; *dash-dot line*, experimental) from the FWD load center: (*a*) gain spectra; (*b*) phase spectra.

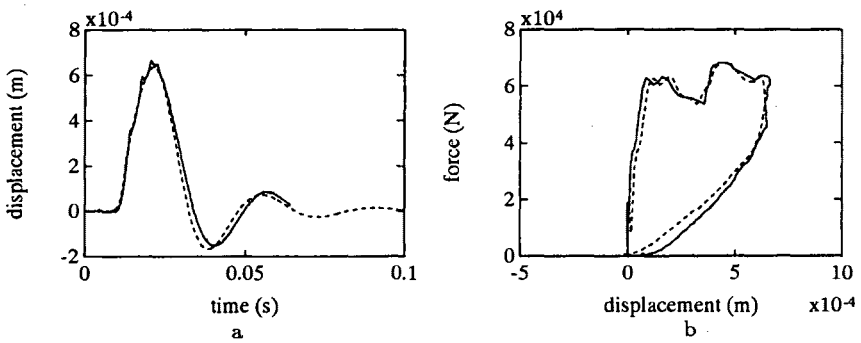

FIGURE 10 Comparison of response predicted using identified model (*dashed line*) for radial distance 30 cm from load center to measured response (*solid line*) at 30.5 cm: (*a*) displacement versus time; (*b*) force versus displacement.

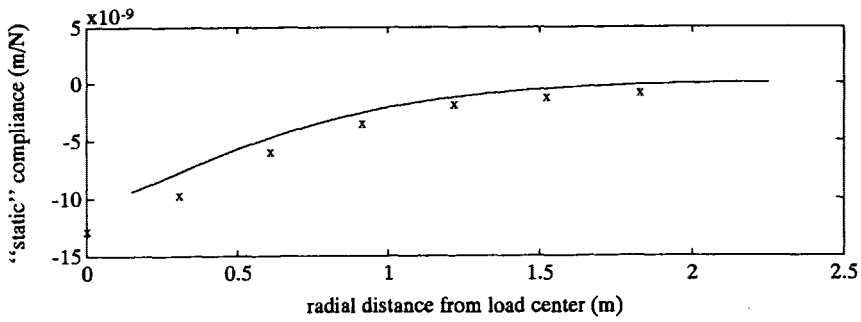

FIGURE 11 Static compliance of pavement as a function of radial distance from load center. *Solid line*: prediction calculated using identified pavement system model; ×, prediction calculated from peak load and displacement values from load cell and geophone data of an FWD test.

ACKNOWLEDGMENTS

E. Kausel of the Massachusetts Institute of Technology provided the software implementation of the thin layer method used for this study. His kind support is sincerely appreciated. Christopher Berini of the U.S. Army Engineer Cold Regions Research and Engineering Laboratory (CRREL) provided capable technical support for the experiments. Funding for this work was provided by the CRREL In-House Laboratory Independent Research Program.

REFERENCES

1. Roesset, J. M., and K.-Y. Shao. Dynamic Interpretation of Dynaflect and Falling Weight Deflectometer Tests. In *Transportation Research Record 1022*, TRB, National Research Council, Washington, D.C., 1985, pp. 7–16.
2. Sebaaly, B., T. Davis, and M. S. Mamlouk. Dynamics of Falling Weight Deflectometer. *Journal of Transportation Engineering*, ASCE, Vol. 110, No. 6, 1985, pp. 618–632.
3. Anderson, M. *Backcalculation of Composite Pavement Layer Moduli*. Technical Report GL-90-15. Army Engineer Waterways Experiment Station, Vicksburg, Miss., 1990.
4. Magnuson, A. H., R. L. Lytton, and R. C. Briggs. Comparison of Computer Predictions and Field Data for Dynamic Analysis of Falling Weight Deflectometer Data. In *Transportation Research Record 1293*, TRB, National Research Council, Washington, D.C., 1991, pp. 61–71.
5. Chang, D-W, Y. V. Kang, J. M. Roesset, and K. H. Stokoe II. Effect of Depth to Bedrock on Deflection Basins Obtained with Dynaflect and FWD Tests. In *Transportation Research Record 1355*, TRB, National Research Council, Washington, D.C., 1992.
6. Dennis, Jr., J. E., and R. B. Schnabel. *Numerical Methods for Unconstrained Optimization and Nonlinear Equations*. Prentice-Hall, Englewood Cliffs, N.J., 1983.
7. Kausel, E., and R. Peek. Dynamic Loads in the Interior of a Layered Stratum: An Explicit Solution. *Bulletin of the Seismological Society of America*, Vol. 72, No. 5, 1982, pp. 1459–1481.
8. Seale, S., and E. Kausel. Point Loads in Cross-Anisotropic Layered Halfspaces. *Journal of Engineering Mechanics*, ASCE, Vol. 115, No. 3, 1989, pp. 509–524.
9. Bendat, J. S., and A. G. Piersol. *Random Data*, 2nd ed. John Wiley and Sons, Inc., New York, 1986.
10. Ewins, D. W. *Modal Testing: Theory and Practice*. John Wiley and Sons, Inc., New York, 1984.
11. Bendat, J. S., and A. G. Piersol. *Engineering Applications of Correlation and Spectral Analysis*. John Wiley and Sons, Inc., New York, 1980.
12. Luco, J. E., and H. L. Wong. Identification of Soil Properties from Foundation Impedance Functions. *Journal of Geotechnical Engineering*, ASCE, Vol. 118, No. 5, 1992, pp. 780–795.
13. Behrens, R. T. *NONLINPK: NESOLVE and UMSOLVE*, Release 1.1. MATLAB User Group Software Archive, NETLIB server, Oak Ridge National Laboratories, 1990.
14. Kausel, E. Wave Propagation in Anisotropic Layered Media. *International Journal for Numerical Methods in Engineering*, Vol. 23, 1986, pp. 1567–1578.
15. Kausel, E. *PUNCH: Program for the Dynamic Analysis of Layered Soils*, Version 3.0. Massachusetts Institute of Technology, 1989.

Publication of this paper sponsored by Committee on Soil and Rock Properties.